Paper

Unified Theory of Non-Resonant and Resonant Circuits in Inductive Power Transfer and Capacitive Power Transfer

Hirono Namiki*a) Non-Member Takehiro Imura* Member Yoichi Hori* Fellow

This paper provides a general and systematic comparison of the transmission characteristics for circuits non-resonant, series resonant and parallel resonant circuits of both Inductive Power Transfer (IPT) and Capacitive Power Transfer (CPT) systems. The transmission characteristics were CC/CV characteristic, efficiency and output power when the power source is a voltage or current source. In terms of the compensation condition and CC/CV characteristic, S-S in IPT and P-P in CPT were superior because the compensation condition does not depend on the coupling coefficient and they had gyrator characteristic. For the efficiency, it was found that, for both IPT and CPT, it was suitable to use S or P on the receiver side for high efficiency. For the output power, in common with IPT and CPT, higher power can be obtained by choosing S on the transmitter side when a voltage source was used and P on the transmitter side when a current source was used. Therefore, it is clear that the circuits with superior compensation condition, CC/CV characteristic, optimal load, efficiency and output power were S-S in IPT when a voltage source was used and P-P in CPT when a current source was used.

Keywords : inductive power transfer, capacitive power transfer, transmission characteristics, circuits

1. Introduction

In recent years, as electronic devices have become more widespread and opportunities for charging have increased year by year. The problems with cable charging include lack of durability, risk of electric shock, cable deterioration and disconnection. All of these problems can be solved by wireless power transfer (WPT).

Inductive Power Transfer (IPT) and Capacitive Power Transfer (CPT) are representative non-radiative methods of WPT. Both have advantage as transmission methods that can achieve higher transmission efficiency than radiative transmission over transmission distances of up to several tens of centimeters. Due to the difference in the main transmission field, they have different characteristics: the advantages of IPT are that it is easier to achieve higher power and longer transmission distances compared to CPT; the advantages of CPT are that there is no risk of efficiency loss or heat generation due to metallic particles and lower cost and weight due to the use of metal plates only. Some previous studies carried out on IPT to compare the characteristics of different circuits(1)(2) and to select circuits suitable for different applications(3)-(8). On the other hand, there are some studies that carried out on CPT to compare the characteristics of different circuits(9)-(11) and to study circuits for high power, which is a problem for CPT (12)-(15). There are series resonance (S) and parallel resonance (P) circuits for IPT and CPT respectively, and typical circuits such as S-S, S-P, P-S and P-P circuits exist by the combining of these circuits. Previous studies compared the four basic circuits of IPT and CPT, but these comparisons were based on only one of the transmission methods and not on comprehensive and fair comparisons, including non-resonance. Furthermore, comparisons have mainly been made with voltage source, with few comparisons of circuits using current source. However, there are situations where current sources are used (16)(17) and by comparing voltage and current sources, the correspondence between IPT and CPT can be found.

Therefore, in this paper, the transmission characteristics compared by solving the circuit equations, which are the basis of electric circuits, to obtain the transmission characteristic equations and substituting the parameters of the unification conditions. For the circuits, the circuits are compared for IPT and CPT respectively, when the transmitter and receiver sides are non-resonant, series resonant and parallel resonant. The transmission characteristics are the CC/CV characteristic, efficiency and output power when the power source is a voltage or current source. Unified conditions are compensation topology based on resonance phenomena, design method for compensation condition, loading condition, Q value, coupling coefficient k and power supply performance.

The remainder of the paper is made up as follows: in Chapter 2, the all compared circuits is presented. In Chapters 3-5, the circuit equations for each circuit are solved and the respective expressions for the power transmission characteristics are derived. Specifically, the compensation condition and constant current (CC) / constant voltage (CV) characteristics are derived in Chapter 3, efficiency and optimal load in Chapter 4 and output power in Chapter 5. In Chapter 6 demonstrates the credibility of the calculations by comparing the calculation with the simulation. In Chapter 7 compares the transmission characteristics for each circuit by fair condition parameters to each equation. A comparison with experiment is made in Chapter 8 and a conclusion is given in Chapter 9.

2. Compared Circuits in IPT and CPT

2.1 Equivalent Circuit in IPT A typical transmission coil is shown in Fig. 1 and its structure can be shown by an

a) Correspondence to: Hirono Namiki. E-mail: namiki.hirono21@gmail.com
* Tokyo University of Science, Imura-Hori Laboratory, 2639, Yamazaki, Noda, Chiba 278-0022, Japan

equivalent circuit as shown in Fig. 2 (a). It can also be transformed into an equivalent T-shaped circuit as shown in Fig 2 (b). Here, the self-inductance and internal resistance of the transmitter coil are L_1 and r_1 respectively, while the self-inductance and internal resistance of the receiver coil are L_2 and r_2 respectively. The mutual inductance L_m, the coupling coefficient k representing the coupling between the transmitter and receiver and the Q values of the coils are defined as in equations (1) and (2).

$$L_m = k\sqrt{L_1 L_2} \quad (1)$$

$$Q_1 = \frac{\omega L_1}{r_1}, Q_2 = \frac{\omega L_2}{r_2} \quad (2)$$

2.2 Equivalent Circuit in CPT A typical transmitter/receiver capacitor consists of four plates as shown in Fig. 3. The self-capacitances C_1, C_2 and the mutual capacitance C_m can be expressed by equations (3)-(6), since each of the four plates is coupled to each other as shown in Fig. 4(a). Therefore, the π-type circuit can be represented as shown in Fig. 4.

$$C_1 = C_{12} + \frac{(C_{13}+C_{14})(C_{23}+C_{24})}{C_{13}+C_{14}+C_{23}+C_{24}} \quad (3)$$

$$C_2 = C_{34} + \frac{(C_{13}+C_{14})(C_{23}+C_{24})}{C_{13}+C_{14}+C_{23}+C_{24}} \quad (4)$$

$$C_m = \frac{C_{24}C_{13}-C_{14}C_{23}}{C_{13}+C_{14}+C_{23}+C_{24}} \quad (5)$$

$$C_m = k\sqrt{C_1 C_2} \quad (6)$$

2.3 Compared Circuits The circuits of IPT and CPT, which are compared in this paper, are shown in Fig. 5 and 6. The circuits consist of a non-resonant circuit (N), in IPT a transmission coil with a resonant capacitor connected in series (S) and in parallel (P), in CPT a transmission capacitor with a resonant coil connected in series, P, connected in parallel are compared.

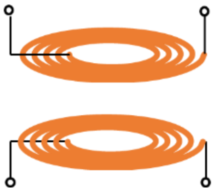

Fig. 1. Transmission Coil in IPT.

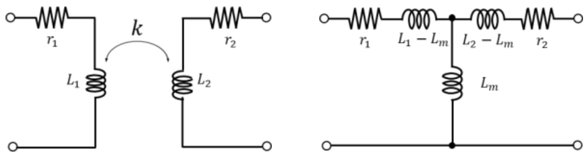

(a)Coupled circuit in IPT (b) T-type circuit

Fig. 2. Equivalent circuit in IPT.

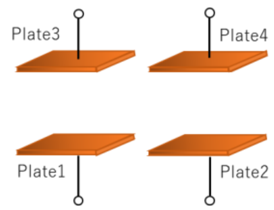

Fig. 3. Transmitter coupler in CPT.

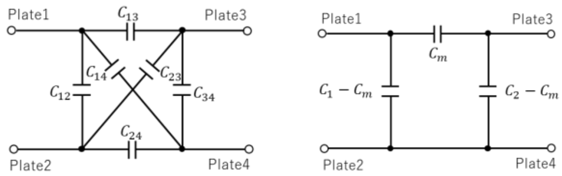

(a) Coupled circuit in CPT (b) π-type circuit

Fig. 4. Equivalent circuit in CPT.

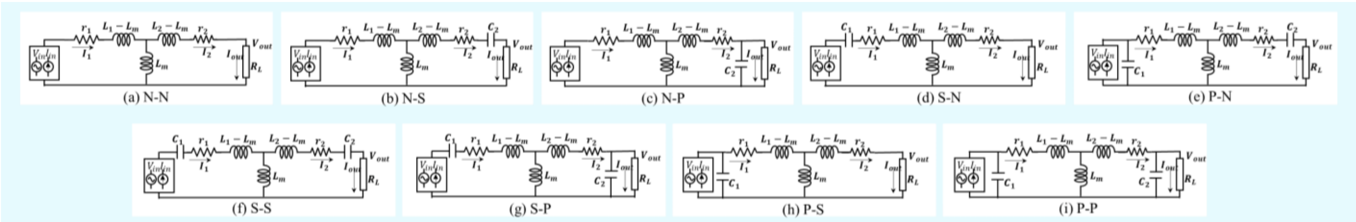

Fig. 5. Compared Circuits in IPT.

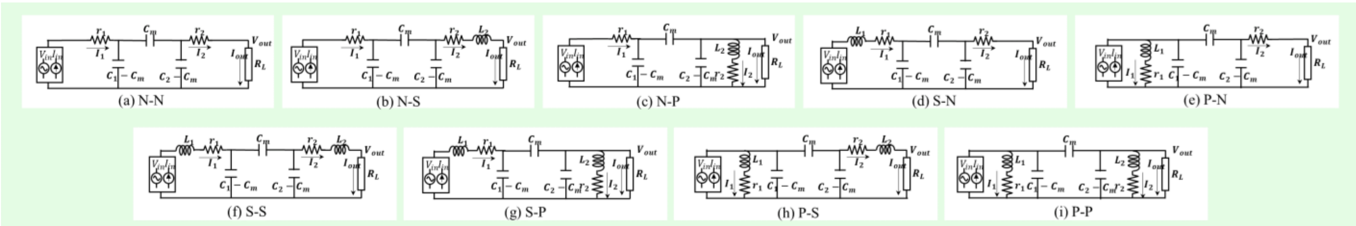

Fig. 6. Compared Circuits in CPT.

3. Compensation Condition and CC/CV Characteristic

3.1 How to Design Compensation Condition In this chapter, the compensation condition and the CC/CV characteristics of resistance load are derived. The compensation elements are resonant capacitors in IPT and resonant inductors in CPT, which can achieve high efficiency and high power by appropriate design. In this paper, the values of reactance compensation elements are determined by a design method based on gyrator or ideal transformer characteristic. The design method based on gyrator or ideal transformer characteristic is a design method in which the F parameter of a two-terminal pair circuit such as equation (7) are set to $A = D = 0$ or $B = C = 0$ under the condition that $r_1 = r_2 = 0$, so that high-efficiency transmission can be achieved.

$$\begin{bmatrix} V_{in} \\ I_{in} \end{bmatrix} = \begin{bmatrix} A & B \\ C & D \end{bmatrix} \begin{bmatrix} V_{out} \\ I_{out} \end{bmatrix} \quad (7)$$

$$\begin{bmatrix} V_{in} \\ I_{in} \end{bmatrix} = \begin{bmatrix} 0 & \pm jZ_0 \\ \pm j\frac{1}{Z_0} & 0 \end{bmatrix} \begin{bmatrix} V_{out} \\ I_{out} \end{bmatrix} \quad (8)$$

$$\begin{bmatrix} V_{in} \\ I_{in} \end{bmatrix} = \begin{bmatrix} \pm jZ_0 & 0 \\ 0 & \pm j\frac{1}{Z_0} \end{bmatrix} \begin{bmatrix} V_{out} \\ I_{out} \end{bmatrix} \quad (9)$$

3.2 Compensation Condition and CC/CV Characteristic in IPT The F parameter of S-S circuit in IPT can be expressed as in equation (10).

$$\begin{cases} A = \frac{1}{j\omega L_m}\left(j\omega L_1 + \frac{1}{j\omega C_1}\right) \\ B = \frac{1}{j\omega L_m}\left\{\left(j\omega L_1 + \frac{1}{j\omega C_1}\right)\left(j\omega L_2 + \frac{1}{j\omega C_2}\right) - \omega^2 L_m^2\right\} \\ C = \frac{1}{j\omega L_m} \\ D = \frac{1}{j\omega L_m}\left(j\omega L_2 + \frac{1}{j\omega C_2}\right) \end{cases} \quad (10)$$

By proper design of the compensation capacitor, it is possible to satisfy $A = D = 0$, in which case C_1 and C_2 are as in equation (11). Furthermore, the F parameter can be represented as in equation (12).

$$C_1 = \frac{1}{\omega^2 L_1}, C_2 = \frac{1}{\omega^2 L_2} \quad (11)$$

$$\begin{bmatrix} V_{in} \\ I_{in} \end{bmatrix} = \begin{bmatrix} 0 & j\omega L_m \\ \frac{1}{j\omega L_m} & 0 \end{bmatrix} \begin{bmatrix} V_{out} \\ I_{out} \end{bmatrix} \quad (12)$$

Equation (12) shows that the resistance load of S-S in IPT has a constant current characteristic when the power supply is a voltage source and a constant voltage characteristic when a current source is used due to gyrator characteristic.

Table 1. shows the results of the compensation condition. The compensation conditions of S-P, P-S and P-P circuits depend on the coupling coefficient k. Therefore, it is not suitable when the coupling coefficient varies. Table 2. shows the results of CC/CV characteristics. The circuits including non-resonance do not have CC/CV characteristic, depending on the type of power supply.

Table 1. Compensation condition in IPT.

Circuit	C_1	C_2
N-N	None	None
N-S	None	$C_2 = \frac{1}{\omega^2 L_2}$
N-P	None	$C_2 = \frac{1}{\omega^2 L_2}$
S-N	$C_1 = \frac{1}{\omega^2 L_1}$	None
P-N	$C_1 = \frac{1}{\omega^2 L_1}$	None
S-S	$C_1 = \frac{1}{\omega^2 L_1}$	$C_2 = \frac{1}{\omega^2 L_2}$
S-P	$C_1 = \frac{1}{\omega^2 (1-k^2) L_1}$	$C_2 = \frac{1}{\omega^2 L_2}$
P-S	$C_1 = \frac{1}{\omega^2 L_1}$	$C_2 = \frac{1}{\omega^2 (1-k^2) L_2}$
P-P	$C_1 = \frac{1}{\omega^2 (1-k^2) L_1}$	$C_2 = \frac{1}{\omega^2 (1-k^2) L_2}$

Table 2. CC/CV characteristic in IPT.

Circuit	Voltage Source	Current Source
N-N	None	None
N-S	None	CV
N-P	None	CC
S-N	CC	None
P-N	None	CC
S-S	CC	CV
S-P	CV	CC
P-S	CV	CC
P-P	CC	CV

3.3 Compensation Condition and CC/CV Characteristic in CPT As with CPT, the compensation condition and CC/CV characteristic are obtained using S-S circuit as an example. The F parameter of S-S circuit can be expressed by equation (13).

$$\begin{cases} A = \frac{1}{C_m}\{C_2 - \omega^2 L_1 (C_1 C_2 - C_m^2)\} \\ B = \frac{1}{j\omega C_m}\{\omega^4 L_1 L_2 C_m^2 + (1 - \omega^2 L_1 C_1)(1 - \omega^2 L_2 C_2)\} \\ C = \frac{j\omega}{C_m}(C_1 C_2 - C_m^2) \\ D = \frac{1}{C_m}\{C_1 - \omega^2 L_2 (C_1 C_2 - C_m^2)\} \end{cases} \quad (13)$$

By proper design of the compensation capacitor, it is possible to satisfy $A = D = 0$, in which case L_1 and L_2 are as in equation (14). Furthermore, the F parameter can be represented as in equation (15).

$$L_1 = \frac{1}{\omega^2 (1-k^2) C_1}, L_2 = \frac{1}{\omega^2 (1-k^2) C_2} \quad (14)$$

$$\begin{bmatrix} V_{in} \\ I_{in} \end{bmatrix} = \begin{bmatrix} 0 & \frac{\omega^4 L_1 L_2 C_m^2 + (1-\omega^2 L_1 C_1)(1-\omega^2 L_2 C_2)}{j\omega C_m} \\ \frac{j\omega (C_1 C_2 - C_m^2)}{C_m} & 0 \end{bmatrix} \begin{bmatrix} V_{out} \\ I_{out} \end{bmatrix} \quad (15)$$

Table 3. Compensation condition in CPT.

Circuit	L_1	L_2
N-N	None	None
N-S	None	$L_2=\frac{1}{\omega^2 C_2}$
N-P	None	$L_2=\frac{1}{\omega^2 C_2}$
S-N	$L_1=\frac{1}{\omega^2 C_1}$	None
P-N	$L_1=\frac{1}{\omega^2 C_1}$	None
S-S	$L_1=\frac{1}{\omega^2(1-k^2)C_1}$	$L_2=\frac{1}{\omega^2(1-k^2)C_2}$
S-P	$L_1=\frac{1}{\omega^2 C_1}$	$L_2=\frac{1}{\omega^2(1-k^2)C_2}$
P-S	$L_1=\frac{1}{\omega^2(1-k^2)C_1}$	$L_2=\frac{1}{\omega^2 C_2}$
P-P	$L_1=\frac{1}{\omega^2 C_1}$	$L_2=\frac{1}{\omega^2 C_2}$

Table 4. CC/CV characteristic in CPT.

Circuit	Voltage Source	Current Source
N-N	None	None
N-S	CC	None
N-P	CC	None
S-N	None	CV
P-N	None	CV
S-S	CC	CV
S-P	CV	CC
P-S	CV	CC
P-P	CC	CV

Equation (15) shows that the resistance load of S-S in CPT has a constant current characteristic when the power supply is a voltage source and a constant voltage characteristic when a current source is used due to gyrator characteristic.

Table 3. shows the results of the compensation condition. The compensation conditions of S-S, S-P and P-S circuits depend on the coupling coefficient k. Therefore, it is not suitable when coupling coefficient varies. Table 4. shows the results of CC/CV characteristics. The circuits including non-resonance do not have CC/CV characteristic, depending on the type of power supply.

4. Efficiency and Optimal Load

4.1 Type of Power Supply and Efficiency This chapter derives the equations for efficiency and optimal load in each circuit. The equations for efficiency and optimal load do not depend on the type of power supply, so for simplicity, a voltage source is used to obtain the equations. The reason why it does not depend on the type of power supply is that the value of the power supply does not affect the efficiency when a load resistance is used, and the input voltage V_{in} and input current I_{in} have a relationship as shown in equation (16) using the input impedance Z_{in}.

$$|V_{in}| = |Z_{in}||I_{in}| \quad (16)$$

Since, since voltage and current sources are interchangeable, it can be said that the efficiency is independent of the type of power supply and the optimal load determined from the efficiency is also independent of the type of power supply.

4.2 Efficiency and Optimal Load in IPT When the above compensation capacitor conditions are applied, the circuit equation of S-S circuit is as in equation (17) when the loop currents I_{l1} and I_{l2} are set as shown in Fig. 7.

$$\begin{bmatrix} V_{in} \\ 0 \end{bmatrix} = \begin{bmatrix} r_1 & -j\omega L_m \\ -j\omega L_m & r_2+R_L \end{bmatrix} \begin{bmatrix} I_{l1} \\ I_{l2} \end{bmatrix} \quad (17)$$

As the matrix determinant is Δ, the currents are as in equations (18), (19).

$$I_1 = I_{l1} = \frac{V_{in}}{\Delta}(r_2+R_L) \quad (18)$$

$$I_2 = I_{out} = I_{l2} = \frac{V_{in}}{\Delta} j\omega L_m \quad (19)$$

Since the efficiency η can be obtained from equation (20), the respective ratios can be taken as in equation (21). Using Q_1 and Q_2 from equation (2), the efficiency is given by equation (22).

$$\eta = \frac{R_L|I_{out}|^2}{r_1|I_1|^2+r_2|I_2|^2+R_L|I_{out}|^2} \quad (20)$$

$$r_1|I_1|^2 : r_2|I_2|^2 : R_L|I_{out}|^2 = r_1(r_2+R_L)^2 : \omega^2 L_m^2 r_2 : \omega^2 L_m^2 R_{out} \quad (21)$$

$$\eta^{S-S} = \frac{k^2 Q_1 Q_2 r_2 R_L}{\{(1+k^2 Q_1 Q_2)r_2+R_L\}(r_2+R_L)} \quad (22)$$

In the same way, the efficiency of the other circuits in IPT can be obtained as shown in Table 5.

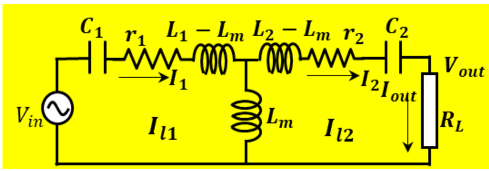

Fig. 7. S-S circuit in IPT.

Table 5. Efficiency in IPT.

Circuit	Efficiency
N-N	$\frac{k^2Q_1Q_2r_2R_L}{\{(1+k^2Q_1Q_2)r_2+R_L\}(r_2+R_L)+Q_2^2r_2^2}$
N-S	$\frac{k^2Q_1Q_2r_2R_L}{\{(1+k^2Q_1Q_2)r_2+R_L\}(r_2+R_L)}$
N-P	$\frac{k^2Q_1^3Q_2^3r_2R_L}{(1+Q_1^2+k^2Q_1Q_2)\{(1+k^2Q_1Q_2)(Q_2^2r_2^2+R_L^2)+Q_2^2r_2R_L\} +(1+Q_1^2)Q_2^2r_2\{Q_2^2r_2+(1+k^2Q_1Q_2)R_L\}}$
S-N	$\frac{k^2Q_1Q_2r_2R_L}{\{(1+k^2Q_1Q_2)r_2+R_L\}(r_2+R_L)+Q_2^2r_2^2}$
P-N	$\frac{k^2Q_1Q_2r_2R_L}{\{(1+k^2Q_1Q_2)r_2+R_L\}(r_2+R_L)+Q_2^2r_2^2}$
S-S	$\frac{k^2Q_1Q_2r_2R_L}{\{(1+k^2Q_1Q_2)r_2+R_L\}(r_2+R_L)}$
S-P	$\frac{k^2(1-k^2)^2Q_1Q_2^3((1-k^2)^2Q_2^2r_2^2+R_L^2)r_2R_L}{\{(1-k^2)^2Q_2^2r_2^2+R_L^2+(1-k^2)^2Q_2^2r_2R_L\} \{(1+k^2Q_1Q_2)\{(1-k^2)^2Q_2^2r_2^2+R_L^2\}+(1-k^2)^2Q_2^2r_2R_L\}+Q_2^2\{(1-k^2)^2Q_2^2r_2^2+k^2R_L^2\}^2}$
P-S	$\frac{k^2Q_1Q_2r_2R_L}{\{(1+k^2Q_1Q_2)r_2+R_L\}(r_2+R_L)+k^4Q_2^2r_2^2}$
P-P	$\frac{k^2(1-k^2)^2Q_1Q_2^3r_2R_L\{(1-k^2)^2Q_2^2r_2^2+R_L^2\}}{\{(1-k^2)^2Q_2^2r_2(r_2+R_L)+R_L^2\} [(1+k^2Q_1Q_2)\{(1-k^2)^2Q_2^2r_2^2+R_L^2\}+(1-k^2)^2Q_2^2r_2R_L]+Q_2^2\{(1-k^2)^2Q_2^2r_2^2+k^2R_L^2\}^2}$

Table 6. Optimal load in IPT.

Circuit	Optimal Load
N-N	$r_2\sqrt{1+Q_2^2+k^2Q_1Q_2}$
N-S	$r_2\sqrt{1+k^2Q_1Q_2}$
N-P	$Q_2r_2\sqrt{\frac{(1+Q_1^2)(1+Q_2^2+k^2Q_1Q_2)+k^2Q_1Q_2(1+k^2Q_1Q_2)}{(1+k^2Q_1Q_2)(1+Q_1^2+k^2Q_1Q_2)}}$
S-N	$r_2\sqrt{1+Q_2^2+k^2Q_1Q_2}$
P-N	$r_2\sqrt{1+Q_2^2+k^2Q_1Q_2}$
S-S	$r_2\sqrt{1+k^2Q_1Q_2}$
S-P	$(1-k^2)Q_2r_2\sqrt{\frac{1+Q_2^2+k^2Q_1Q_2}{1+k^2Q_1Q_2+k^4Q_2^2}}$
P-S	$r_2\sqrt{1+k^2Q_1Q_2+k^4Q_2^2}$
P-P	$(1-k^2)Q_2r_2\sqrt{\frac{1+Q_2^2+k^2Q_1Q_2}{1+k^2Q_1Q_2+k^4Q_2^2}}$

The optimal load R_{Lopt} to achieve maximum efficiency in S-S circuit can be obtained equation (24) by applying the differential equation in equation (23) to equation (22).

$$\frac{\partial \eta}{\partial R_L}=0 \quad \cdots\cdots (23)$$

$$R_{Lopt}^{S-S}=r_2\sqrt{1+k^2Q_1Q_2} \quad \cdots\cdots (24)$$

In the same way, the optimal load for the other circuits in IPT is calculated as shown in Table 6.

4.3 Efficiency and Optimal Load in CPT The efficiency can be obtained by solving the circuit equations by applying the aforementioned compensation inductor conditions. The circuit equation of S-S circuit in CPT is as in equation (25) when the loop currents I_{l1}, I_{lm} and I_{l2} are set as in Fig 8. Here, δ_k, C_1', C_2' are defined according to equation (26).

$$\begin{bmatrix} V_{in} \\ 0 \\ 0 \end{bmatrix}=\begin{bmatrix} r_1+\frac{-\delta_k+\omega^2L_1C_m}{j\omega C_1'} & \frac{1}{j\omega C_1'} & 0 \\ -\frac{1}{j\omega C_1'} & \frac{C_1C_2-C_m^2}{j\omega C_1'C_2'C_m} & \frac{1}{j\omega C_2'} \\ 0 & \frac{1}{j\omega C_2'} & r_2+R_L+\frac{-\delta_k+\omega^2L_2C_m}{j\omega C_2'} \end{bmatrix}\begin{bmatrix} I_{l1} \\ I_{lm} \\ I_{l2} \end{bmatrix} \cdot (25)$$

$$\delta_k=\frac{k^2}{1-k^2}, C_1'=(C_1-C_m), C_2'=C_2-C_m \quad \cdots\cdots (26)$$

As the matrix determinant is Δ, the currents are as in equations (27), (28).

$$I_1=I_{l1}=\frac{V_{in}}{\Delta}\left\{\frac{C_1C_2-C_m^2}{j\omega C_1'C_2'C_m}\left(r_2+R_L+\frac{-\delta_k+\omega^2L_2C_m}{j\omega C_2'}\right)+\frac{1}{\omega^2C_2'^2}\right\} \cdots\cdots (27)$$

$$I_2=I_{out}=I_{l2}=\frac{V_{in}}{\Delta}\frac{1}{\omega^2C_1'C_2'} \quad \cdots\cdots (28)$$

Since the efficiency is obtained from equation (20), the ratio of each can be taken as equation (29), and the efficiency can be expressed as equation (30) by using the Q value given in equation (2) for the resonant coil.

$$r_1|I_1|^2 : r_2|I_2|^2 : R_L|I_{out}|^2=(C_1C_2-C_m^2)^2(r_2+R_L)^2 : C_m^2r_2 : C_m^2R_L \cdot (29)$$

$$\eta^{S-S}=\frac{k^2Q_1Q_2r_2R_L}{\{(1+k^2Q_1Q_2)r_2+R_L\}(r_2+R_L)} \quad \cdots\cdots (30)$$

Similarly, the efficiencies for the other circuits in CPT can be obtained as shown in Table 7.

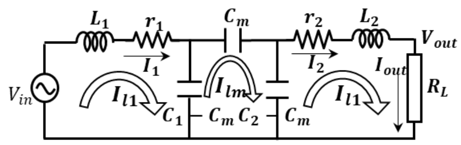

Fig. 8. S-S circuit in CPT.

Table 7. Efficiency in CPT.

Circuit	Efficiency
N-N	$\frac{k^2Q_1Q_2r_2R_L}{[\{(1-k^2)^2+k^2Q_1Q_2\}r_2+(1-k^2)^2R_L](r_2+R_L)+Q_2^2r_2^2}$
N-S	$\frac{k^2Q_1Q_2r_2R_L}{[\{(1-k^2)^2+k^2Q_1Q_2\}r_2+(1-k^2)^2R_L](r_2+R_L)+k^4Q_2^2r_2^2}$
N-P	$\frac{k^2Q_1Q_2[\{(1+Q_2^2)r_2+R_L\}^2+Q_2^2R_L^2]r_2R_L}{Q_2^2\{Q_2^2r_2^2+(r_2+R_L)^2-(1-k^2)R_L^2\}^2 +\{(1+Q_2^2)r_2+R_L\}[(1-k^2)^2\{(1+Q_2^2)r_2+R_L\}R_L+k^2Q_1Q_2\{(r_2+R_L)^2+Q_2^2r_2^2\}]R_L}$
S-N	$\frac{k^2Q_1Q_2r_2R_L}{[\{(1-k^2)^2+k^2Q_1Q_2\}r_2+(1-k^2)^2R_L](r_2+R_L)+Q_2^2r_2^2}$
P-N	$\frac{k^2Q_1Q_2r_2R_L}{[\{(1-k^2)^2+k^2Q_1Q_2\}r_2+(1-k^2)^2R_L](r_2+R_L)+Q_2^2r_2^2}$
S-S	$\frac{k^2Q_1Q_2r_2R_L}{\{(1+k^2Q_1Q_2)r_2+R_L\}(r_2+R_L)}$
S-P	$\frac{k^2Q_1Q_2[\{(1+Q_2^2)r_2+R_L\}^2+Q_2^2R_L^2]r_2R_L}{(1-k^2)^2Q_2^2r_2^2\{(1+Q_2^2)r_2+2R_L\}^2 +\{(1+Q_2^2)r_2+R_L\}R_L[(1-k^2)\{(1+Q_2^2)r_2+R_L\}R_L+k^2Q_1Q_2\{(r_2+R_L)^2+Q_2^2r_2^2\}]}$
P-S	$\frac{k^2Q_1Q_2r_2R_L}{[\{(1-k^2)^2+k^2Q_1Q_2\}r_2+(1-k^2)R_L](r_2+R_L)+k^4Q_2^2r_2^2}$
P-P	$\frac{k^2Q_1Q_2[\{(1+Q_2^2)r_2+R_L\}^2+Q_2^2R_L^2]r_2R_L}{Q_2^2\{Q_2^2r_2^2+(r_2+R_L)^2-(1-k^2)R_L^2\}^2 +\{(1+Q_2^2)r_2+R_L\}[(1-k^2)^2\{(1+Q_2^2)r_2+R_L\}R_L+k^2Q_1Q_2\{(r_2+R_L)^2+Q_2^2r_2^2\}]R_L}$

The optimal load R_{Lopt} to achieve maximum efficiency in S-S circuit can be obtained by applying the differential equation in equation (23) to equation (31).

$$R_{Lopt}^{S-S}=r_2\sqrt{1+k^2Q_1Q_2} \quad \cdots\cdots (31)$$

In the same way, the optimal load for the other circuits of CPT is calculated as shown in Table 8.

Table 8. Optimal load in CPT.

Circuit	Optimal Load
N-N	$\frac{r_2}{1-k^2}\sqrt{(1-k^2)^2+Q_2^2+k^2Q_1Q_2}$
N-S	$\frac{r_2}{1-k^2}\sqrt{(1-k^2)^2+k^4Q_2^2+k^2Q_1Q_2}$
N-P	$Q_2r_2\sqrt{\frac{1+Q_2^2}{(1-k^2)^2+k^4Q_2^2+k^2Q_1Q_2}}$
S-N	$\frac{r_2}{1-k^2}\sqrt{(1-k^2)^2+Q_2^2+k^2Q_1Q_2}$
P-N	$\frac{r_2}{1-k^2}\sqrt{(1-k^2)^2+Q_2^2+k^2Q_1Q_2}$
S-S	$r_2\sqrt{1+k^2Q_1Q_2}$
S-P	$Q_2r_2\sqrt{\frac{(1-k^2)(1+Q_2^2)}{1-k^2+k^2Q_1Q_2}}$
P-S	$r_2\sqrt{\frac{(1-k^2)^2+k^2Q_1Q_2+k^4Q_2^2}{(1-k^2)^2}}$
P-P	$Q_2r_2\sqrt{\frac{1+Q_2^2}{(1-k^2)^2+k^4Q_2^2+k^2Q_1Q_2}}$

5. Output Power

5.1 Output Power in IPT The F parameter of S-S circuit in IPT can be expressed by equation (32).

$$\begin{cases} A = \frac{r_1}{j\omega L_m} \\ B = r_1 r_2 + \omega^2 L_m^2 \\ C = \frac{1}{j\omega L_m} \\ D = \frac{r_2}{j\omega L_m} \end{cases} \quad \cdots\cdots (32)$$

Since equations (33) can be established for V_{out} and I_{out}, the input voltage V_{in} can be expressed from equations (32) and (33) as in equation (34). The output power P_{out} when a voltage source is used can be obtained from equation (35), so that P_{out_Vin} in S-S circuit can be expressed as in equation (36).

$$V_{out} = R_L I_{out} \quad \cdots\cdots (33)$$

$$V_{in} = \frac{I_{out}}{j\omega L_m}\{r_1(r_2 + R_L) + \omega^2 L_m^2\} \quad \cdots\cdots (34)$$

$$P_{out} = R_L |I_{out}|^2 \quad \cdots\cdots (35)$$

$$P_{out\_Vin}^{S-S} = \frac{k^2 Q_1 Q_2 r_2 R_L |V_{in}|^2}{r_1\{(1+k^2 Q_1 Q_2) r_2 + R_L\}^2} \quad \cdots\cdots (36)$$

In the same way, the equation for the output power when a voltage source is connected for the other circuits can be obtained as shown in Table 9.

Furthermore, as the input current I_{in} is expressed by equation (37), the output power P_{out} when using a current source can be obtained from equations (32) and (37) from equation (38). Therefore, P_{out_Iin} in S-S circuit is given by equation (39).

$$I_{in} = \frac{V_{out}}{j\omega L_m}\left(1 + \frac{r_2}{R_L}\right) \quad \cdots\cdots (37)$$

$$P_{out} = \frac{|V_{out}|^2}{R_L} \quad \cdots\cdots (38)$$

$$P_{out\_Iin}^{S-S} = \frac{k^2 Q_1 Q_2 r_1 r_2 R_L |I_{in}|^2}{(r_2+R_L)^2} \quad \cdots\cdots (39)$$

The results of the output power for the other circuits in the same way are shown in Table 10.

Table 9. Output power connecting voltage source in IPT.

Circuit	Output power connecting voltage source
N-N	$\frac{k^2 Q_1 Q_2 r_2 R_L \lvert V_{in}\rvert^2}{r_1[\{(1 - Q_1 Q_2 + k^2 Q_1 Q_2) r_2 + R_L\}^2 + \{(Q_1 + Q_2) r_2 + Q_1 R_L\}^2]}$
N-S	$\frac{k^2 Q_1 Q_2 r_2 R_L \lvert V_{in}\rvert^2}{r_1[\{(1 + k^2 Q_1 Q_2) r_2 + R_L\}^2 + Q_1^2 (r_2 + R_L)^2]}$
N-P	$\frac{k^2 Q_1 Q_2^3 r_2 R_L \lvert V_{in}\rvert^2}{r_1\left[\begin{matrix}\{(1 - Q_1 Q_2 + k^2 Q_1 Q_2) Q_2 r_2 - Q_1 R_L\}^2 \\ +\{(Q_1 + Q_2) Q_2 r_2 + (1 + k^2 Q_1 Q_2) R_L\}^2\end{matrix}\right]}$
S-N	$\frac{k^2 Q_1 Q_2 r_2 R_L \lvert V_{in}\rvert^2}{[\{(1 + k^2 Q_1 Q_2) r_2 + R_L\}^2 + Q_2^2 r_2^2] r_1}$
P-N	$\frac{k^2 Q_1 Q_2 r_2 R_L \lvert V_{in}\rvert^2}{r_1[\{(1 - Q_1 Q_2 + k^2 Q_1 Q_2) r_2 + R_L\}^2 + \{(Q_1 + Q_2) r_2 + Q_1 R_L\}^2]}$
S-S	$\frac{k^2 Q_1 Q_2 r_2 R_L \lvert V_{in}\rvert^2}{r_1\{(1 + k^2 Q_1 Q_2) r_2 + R_L\}^2}$
S-P	$\frac{k^2 Q_1 Q_2^3 r_2 R_L \lvert V_{in}\rvert^2}{r_1[\{Q_2^2 r_2 + R_L + k^2 Q_1 Q_2 (r_2 + R_L)\}^2 + (Q_2 r_2 - k^2 Q_1 R_L)^2]}$
P-S	$\frac{k^2 Q_1 Q_2 r_2 R_L \lvert V_{in}\rvert^2}{r_1[(r_2 + R_L)^2 + \{(Q_1 + k^2 Q_2) r_2 + Q_1 R_L\}^2]}$
P-P	$\frac{k^2 (1 - k^2)^2 Q_1 Q_2^3 r_2 R_L \lvert V_{in}\rvert^2}{r_1\left(\begin{matrix}[(1 - k^2)\{1 - (1 - k^2) Q_1 Q_2\} Q_2 r_2 - \{(1 - k^2) Q_1 + k^2 Q_2\} R_L]^2 \\ +[(1 - k^2)(Q_1 + Q_2) Q_2 r_2 + \{1 - k^2 (1 + k^2 Q_1 Q_2)\} R_L]^2\end{matrix}\right)}$

Table 10. Output power connecting current source in IPT.

Circuit	Output power connecting current source
N-N	$\frac{k^2 Q_1 Q_2 r_1 r_2 R_L \lvert I_{in}\rvert^2}{(r_2 + R_L)^2 + Q_2^2 r_2^2}$
N-S	$\frac{k^2 Q_1 Q_2 r_1 r_2 R_L \lvert I_{in}\rvert^2}{(r_2 + R_L)^2}$
N-P	$\frac{k^2 Q_1 Q_2^3 r_1 r_2 R_L \lvert I_{in}\rvert^2}{Q_2^2 r_2^2 + (Q_2^2 r_2 + R_L)^2}$
S-N	$\frac{k^2 Q_1 Q_2 r_1 r_2 R_L \lvert I_{in}\rvert^2}{(r_2 + R_L)^2 + Q_2^2 r_2^2}$
P-N	$\frac{k^2 Q_1^3 Q_2 r_1 r_2 R_L \lvert I_{in}\rvert^2}{\{(1 + k^2 Q_1 Q_2) r_2 + R_L\}^2 + Q_2^2 r_2^2}$
S-S	$\frac{k^2 Q_1 Q_2 r_1 r_2 R_L \lvert I_{in}\rvert^2}{(r_2 + R_L)^2}$
S-P	$\frac{k^2 Q_1 Q_2^3 r_1 r_2 R_L \lvert I_{in}\rvert^2}{r_2^2 + (Q_2^2 r_2 + R_L)^2}$
P-S	$\frac{k^2 Q_1^3 Q_2 r_1 r_2 R_L \lvert I_{in}\rvert^2}{\{(1 + k^2 Q_1 Q_2) r_2 + R_L\}^2 + k^4 Q_2^2 r_2^2}$
P-P	$\frac{k^2 (1 - k^2) Q_1^3 Q_2^3 r_1 r_2 R_L \lvert I_{in}\rvert^2}{\begin{matrix}[(1 - k^2)(k^2 Q_1 + Q_2) Q_2 r_2 + \{1 + k^2 (1 - k^2) Q_1 Q_2\} R_L]^2 \\ +\{(1 - k^2) Q_2 r_2 - k^2 (Q_1 + Q_2) R_L\}^2\end{matrix}}$

5.2 Output Power in CPT The F parameter of S-S circuit in CPT can be expressed as in equation (40).

$$\begin{cases} A = -j\omega C_m (r_1 + j\omega L_1) + \frac{C_2}{C_m}(-\delta_k + j\omega C_1 r_1) \\ B = -j\omega C_m (r_1 + j\omega L_1)(r_2 + j\omega L_2) + \frac{1}{j\omega C_m}(-\delta_k + j\omega C_1 r_1)(-\delta_k + j\omega C_2 r_2) \\ C = -j\omega C_m + \frac{j\omega C_1 C_2}{C_m} \\ D = -j\omega C_m (r_2 + j\omega L_2) + \frac{C_1}{C_m}(-\delta_k + j\omega C_2 r_2) \end{cases} \cdots (40)$$

In the same way to IPT, the output power when a voltage source is connected can be obtained as in equation (41).

$$P_{out\_Vin}^{S-S} = \frac{k^2 Q_1 Q_2 r_1 r_2 R_L |V_{in}|^2}{r_1\{(1+k^2 Q_1 Q_2) r_2 + R_L\}} \quad \cdots\cdots (41)$$

For the other circuits, the output power when a voltage source is connected is shown in Table 11

Table 11. Output power connecting voltage source in CPT.

Circuit	Output power connecting voltage source
N-N	$\frac{k^2 Q_1 Q_2 r_2 R_L \lvert V_{in}\rvert^2}{r_1[\{(Q_1 + Q_2) r_2 + (1 + Q_1) R_L\}^2 + \{(1 - k^2 - Q_1 Q_2) r_2 + (1 - k^2) R_L\}^2]}$
N-S	$\frac{k^2 Q_1 Q_2 r_2 R_L \lvert V_{in}\rvert^2}{r_1[Q_1^2 (r_2 + R_L)^2 + \{r_2 + (1 - k^2) R_L\}^2]}$
N-P	$\frac{k^2 Q_1 Q_2 (1 + Q_2^2)^2 r_2 R_L \lvert V_{in}\rvert^2}{r_1[\{Q_1 Q_2 (1 + Q_2^2) r_2 - (1 - k^2 - k^2 Q_2^2 - Q_1 Q_2) R_L\}^2 + (Q_1 + Q_2)^2 R_L^2]}$
S-N	$\frac{k^2 Q_1 Q_2 r_2 R_L \lvert V_{in}\rvert^2}{r_1[(1 - k^2)^2 (r_2 + R_L)^2 + \{(k^2 Q_1 + Q_2) r_2 + k^2 Q_1 R_L\}^2]}$
P-N	$\frac{k^2 Q_1 Q_2 r_2 R_L \lvert V_{in}\rvert^2}{Q_1^2 r_1 \{Q_2^2 r_2^2 + (r_2 + R_L)^2\}}$
S-S	$\frac{k^2 Q_1 Q_2 r_1 r_2 R_L \lvert V_{in}\rvert^2}{r_1\{(1 + k^2 Q_1 Q_2) r_2 + R_L\}}$
S-P	$\frac{k^2 (1 - k^2) Q_1 Q_2 (1 + Q_2^2)^2 r_2 R_L \lvert V_{in}\rvert^2}{r_1\left[k^4 (1 + Q_2^2)^2 R_L^2 + \{(1 + Q_2^2)\left((1 - k^2) Q_2 r_2 + k^2 Q_1 R_L\right) + (1 - k^2) Q_2 R_L\}^2\right]}$
P-S	$\frac{k^2 Q_2 r_2 R_L \lvert V_{in}\rvert^2}{(1 - k^2) Q_1 r_1 (r_2 + R_L)^2}$
P-P	$\frac{k^2 (1 + Q_2^2)^2 Q_2 r_2 R_L \lvert V_{in}\rvert^2}{Q_1 r_1 [\{(1 + Q_2^2) Q_2 r_2 + R_L\}^2 + R_L^2]}$

Table 12. Output power connecting current source in CPT.

Circuit	Output power connecting current source
N-N	$\frac{k^2 Q_1 Q_2 r_1 r_2 R_L \lvert I_{in}\rvert^2}{(1-k^2)^2 (r_2+R_L)^2 + Q_2^2 r_2^2}$
N-S	$\frac{k^2 Q_1 Q_2 r_1 r_2 R_L \lvert I_{in}^2\rvert}{(1-k^2)^2 (r_2+R_L)^2 + k^4 Q_2^2 r_2^2}$
N-P	$\frac{k^2 Q_1 Q_2 (1+Q_2^2)^2 r_1 r_2 R_L \lvert I_{in}\rvert^2}{\{1-k^2(1+Q_2^2)\}^2 R_L^2 + Q_2^2\{(1+Q_2^2)r_2 + R_L\}^2}$
S-N	$\frac{k^2 Q_1 Q_2 r_1 r_2 R_L \lvert I_{in}\rvert^2}{(1-k^2)^2 (r_2+R_L)^2 + Q_2^2 r_2^2}$
P-N	$\frac{k^2 (1+Q_1^2)^2 Q_1 Q_2 r_1 r_2 R_L \lvert I_{in}\rvert^2}{[(1-k^2-k^2 Q_1^2 - Q_1 Q_2) r_2 + \{1-k^2(1+Q_1^2)\}R_L]^2 + \{(Q_1+Q_2)r_2 + Q_1 R_L\}^2}$
S-S	$\frac{k^2 Q_1 Q_2 r_1 r_2 R_L \lvert I_{in}\rvert^2}{(r_2+R_L)^2}$
S-P	$\frac{k^2 Q_1 Q_2 (1+Q_2^2)^2 r_1 r_2 R_L \lvert I_{in}\rvert^2}{(1-k^2)[Q_2^2\{(1+Q_2^2)r_2 + R_L\}^2 + R_L^2]}$
P-S	$\frac{k^2 (1-k^2)^2 (1+Q_1^2)^2 Q_1 Q_2 r_1 r_2 R_L \lvert I_{in}\rvert^2}{[\{(1-k^2+k^2 Q_1 Q_2)Q_1 + k^2 Q_2\} r_2 + (1-k^2) Q_1 R_L]^2 + (1-k^2)^2 (r_2+R_L)^2}$
P-P	$\frac{k^2 (1+Q_1^2)^2 (1+Q_2^2)^2 Q_1 Q_2 r_1 r_2 R_L}{[(1+Q_2^2) Q_1 Q_2 r_2 + \{k^2(1+Q_1^2)(1+Q_2^2) + Q_1 Q_2 - 1\}R_L]^2 + \{(1+Q_2^2) Q_2 r_2 + (Q_1+Q_2) R_L\}^2} \lvert I_{in}\rvert^2$

The output power when a current source is connected is shown in equation (42).

$$P_{out\_Iin}^{S-S} = \frac{k^2 Q_1 Q_2 r_1 r_2 R_L \lvert I_{in}\rvert^2}{(r_2+R_L)^2} \quad (42)$$

For the other circuits, the output power when a current source is connected is shown in Table 12.

6. Comparison with Simulation

In order to verify that the respective equations for the transmission characteristics equations obtained in Chapters 3-5 are correct, a comparison with the simulation values was performed. The simulation is an electromagnetic simulation using the moment method, the coupler used in the simulation is shown in Fig. 9 and the parameters in Table 13. For a fair comparison, the Q values, the coupling coefficient k and power supply performance were common. In addition, the coupler area was designed to be close in value while the coupling coefficient and Q value were common. Here, from Chapter 3, the resonance conditions for S-P, P-S and P-P in IPT and S-S, S-P and P-S in CPT depend on the coupling coefficient, so the parameters of the resonant capacitor in IPT and the resonant coil in CPT are shown in two different cases. Furthermore, in order to match k and Q in IPT and CPT, an external capacitor are used in addition to the transmission capacitor in CPT.

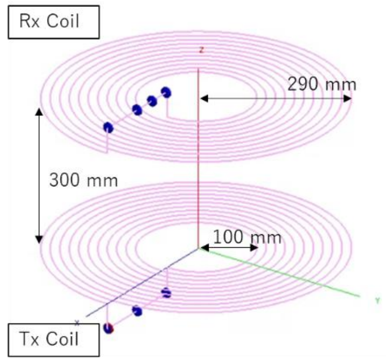

(a) Transmission coil for simulation in IPT

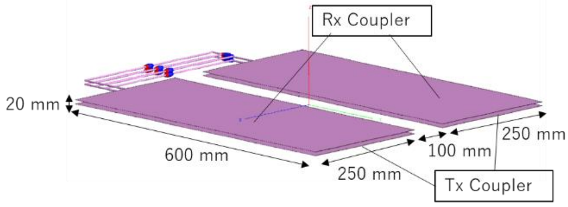

(a) Transmission coupler for simulation in CPT

Fig. 9. Transmission coupler.

Table 13. Parameters of simulation..

	Symbol	Value	
Voltage Source	V_{in}	30 V	
Current Source	I_{in}	1 A	
Coupling Coefficient	k	0.11	
Q value	Q_1, Q_2	231.02	
		IPT	CPT
Resonant Frequency	f	85 kHz	450 kHz
Inductance	L_1, L_2	51.85 µH	independent on k 138.05 µH depend on k 139.76 µH
Internal Resistance	r_1, r_2	0.12 ohm	independent on k 1.69 ohm depend on k 1.71 ohm
Capacitance	C_1, C_2	independent on k 67.62 nF depend on k 68.41 nF	906.08 pF

The results of the calculation and simulation of efficiency and output power are shown in Fig. 10, 11. The output power connecting a current source was converted from the power supply current when a voltage source was connected. Fig. 10, 11 show that the equations derived in Chapter 3-5 are correct, as the calculation and simulation results are in agreement.

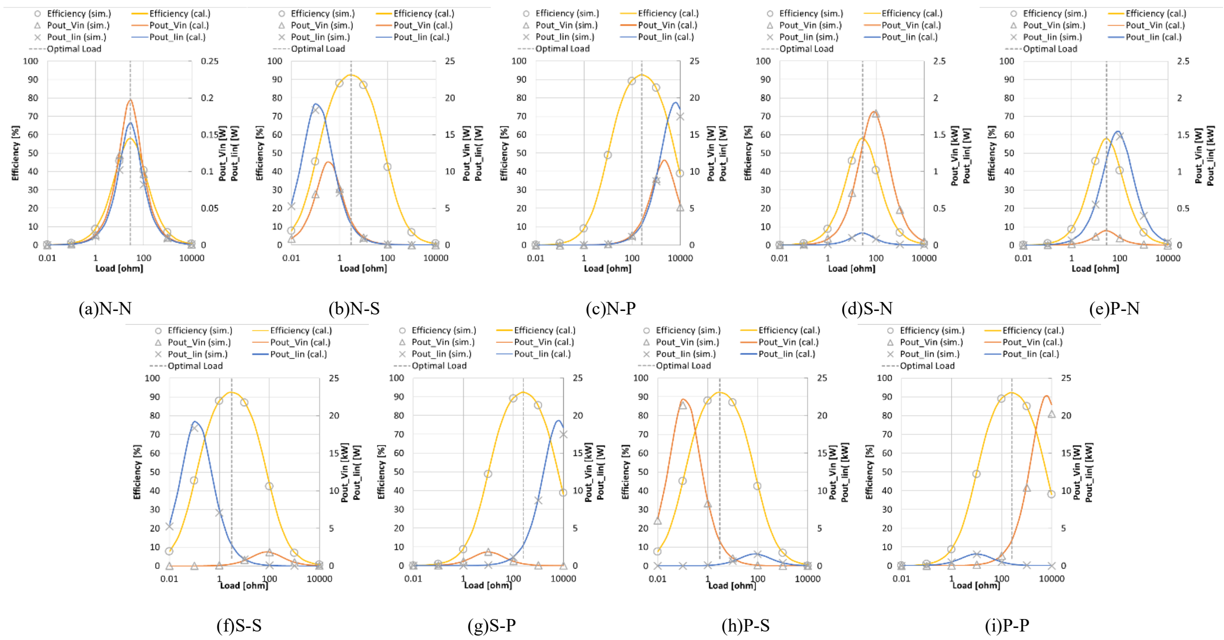

(a)N-N (b)N-S (c)N-P (d)S-N (e)P-N

(f)S-S (g)S-P (h)P-S (i)P-P

Fig. 10 Comparison of simulation and calculation in IPT.

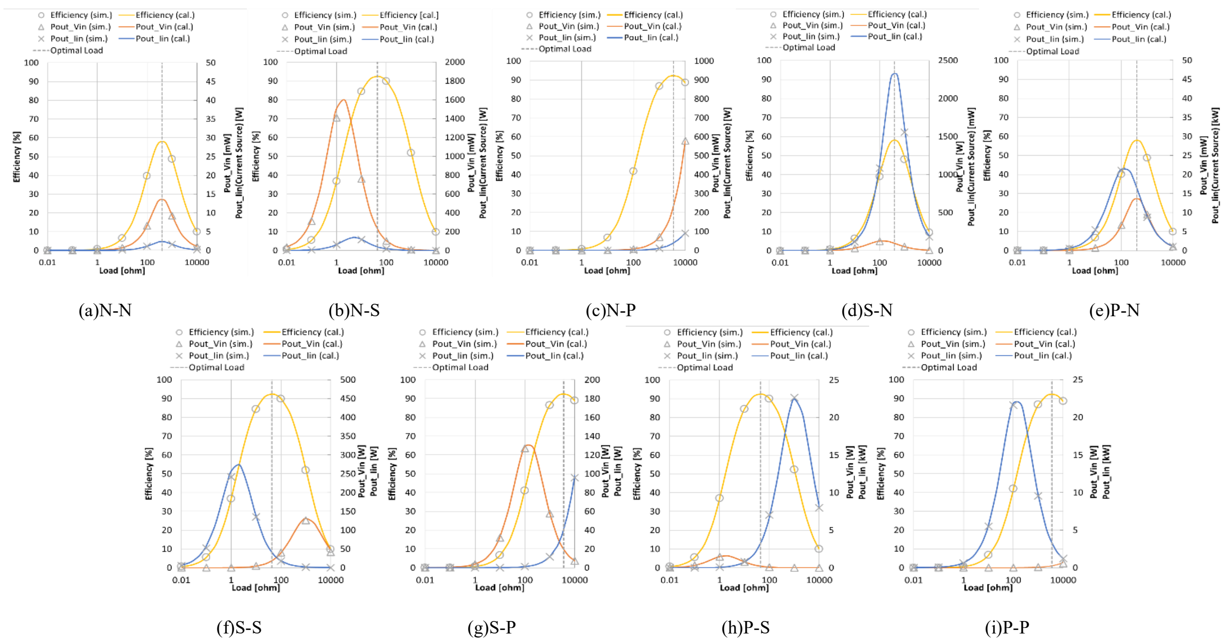

(a)N-N (b)N-S (c)N-P (d)S-N (e)P-N

(f)S-S (g)S-P (h)P-S (i)P-P

Fig. 11 Comparison of simulation and calculation in CPT.

7. Comparison of Transmission Characteristics

The parameters of the unified conditions used in the simulation as shown in Table 13. are substituted into the equation to compare for each transmission characteristic. In addition, the efficiency and output power are compared with the load as the optimal load.

7.1 Optimal Load

For the optimal load, the optimal load for each circuit of IPT and the optimal load for each circuit of CPT are as shown in Fig. 12. From Fig. 12, it is found that the optimal load values for both IPT and CPT depend on the circuit configuration on the receiver side.

Here, using the approximation of equation (43) to the exact equation for the optimal load obtained in Chapter 4, an approximate solution can be obtained as shown in Table 14, regardless of the transmission method.

$$Q_1 = Q_2 = Q, r_1 = r_2 = r, 1 + Q^2 \approx Q^2, 1 + k^2 \approx 1 \cdots (43)$$

Furthermore, under the approximate conditions of equation (44), the optimal load of each circuit is expressed to equation (45).

$$1 + k^2Q^2 \approx k^2Q^2 \cdots\cdots (44)$$

$$R_{Lopt}^{Small} : R_{Lopt}^{Mid} : R_{Lopt}^{Large} = k^2 : k : 1 \cdots\cdots (45)$$

Therefore, when the conditions in equations (43) and (44) are satisfied, the smaller the coupling coefficient, the greater the difference in the value of the optimal load. From the above, it is necessary to select the receiver circuit according to the value of the load.

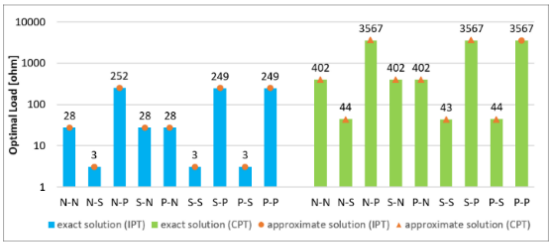

Fig. 12 Optimal load.

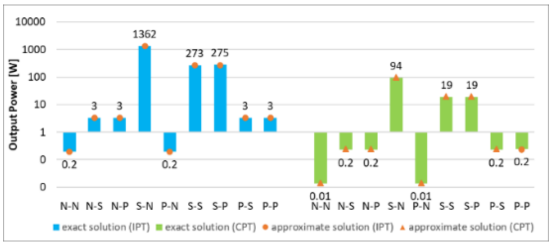

Fig. 14 Output power connecting voltage source.

Table 14. Approximate solution of optimal load.

Transmitter \ Receiver	N	S	P
N	Middle Qr	Small $r\sqrt{1+k^2Q^2}$	Large $\frac{Q^2r}{\sqrt{1+k^2Q^2}}$
S			
P			

Table 16. Approximate solution of output power connecting voltage source.

Transmitter \ Receiver	N	S	P
N	Low $\frac{k^2Q\|V_{in}\|^2}{\{(1+Q)^2+Q^2\}r}$	Middle $\frac{k^2\sqrt{1+k^2Q^2}\|V_{in}\|^2}{r\left(1+\sqrt{1+k^2Q^2}\right)^2}$	
S	Extra High $\frac{k^2Q^3\|V_{in}\|^2}{\{(1+k^2Q^2+Q)^2+Q^2\}r}$	High $\frac{k^2Q^2\|V_{in}\|^2}{r\sqrt{1+k^2Q^2}\left(1+\sqrt{1+k^2Q^2}\right)^2}$	
P	Low $\frac{k^2Q\|V_{in}\|^2}{\{(1+Q)^2+Q^2\}r}$	Middle $\frac{k^2\sqrt{1+k^2Q^2}\|V_{in}\|^2}{r\left(1+\sqrt{1+k^2Q^2}\right)^2}$	

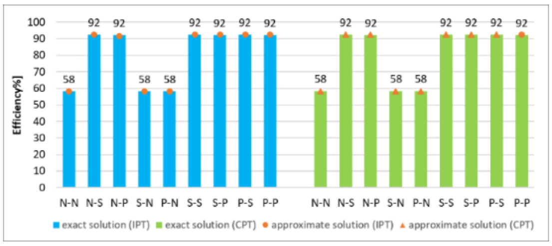

Fig. 13 Maximum Efficiency.

Table 15. Approximate solution of efficiency.

Transmitter \ Receiver	N	S	P
N	Middle $\frac{k^2Q^3}{(1+k^2Q^2+Q)(1+Q)+Q^2}$	High $\frac{k^2Q^2}{\left(1+\sqrt{1+k^2Q^2}\right)^2}$	
S			
P			

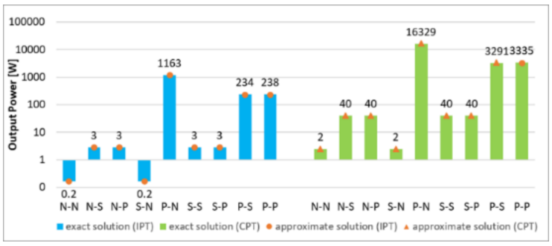

Fig. 15 Output power connecting current source.

Table 17. Approximate solution of output power connecting current source.

Transmitter \ Receiver	N	S	P
N	Low $\frac{k^2Q^3r\|I_{in}\|^2}{(1+Q)^2+Q^2}$	Middle $\frac{k^2Q^2r\sqrt{1+k^2Q^2}\|I_{in}\|^2}{\left(1+\sqrt{1+k^2Q^2}\right)^2}$	
S			
P	Extra High $\frac{k^2Q^5\|I_{in}\|^2}{\{(1+k^2Q^2+Q)^2+Q^2\}r}$	High $\frac{k^2Q^4r\|I_{in}\|^2}{\sqrt{1+k^2Q^2}\left(1+\sqrt{1+k^2Q^2}\right)^2}$	

7.2 Maximum Efficiency

The results for the maximum efficiency at optimal load are shown in Fig. 13, where it can be found that for both IPT and CPT, the efficiency is lower than for the non-resonant circuit N on the receiver side compared to other circuits.

Here, using the approximation of equation (43) to the exact efficiency equation obtained in Chapter 4, and setting the load as Table 14, it can be approximated as Table 15 for IPT and CPT in common. The above shows that for high efficiency transmission, the receiver side should choose S or P, regardless of the transmission method.

7.3 Output Power connecting Voltage Source

The results obtained for the output power when a voltage source is connected shown in Fig. 14. Here, the load value is optimal load.

Fig. 14 shows that the output power is high when the transmitter side is S, and in particular S-N circuit produces the highest power, for both IPT and CPT, Here, using the approximation of equation (43) to the exact equation obtained in Chapter 5, IPT and CPT can be approximated as shown in Table 16. From the above, it can be seen that when a voltage source is connected, high power can be obtained by selecting S circuit for the transmitter side circuit, regardless of the transmission method.

7.4 Output Power connecting Current Source The results obtained for the output power when a current source is connected shown in Fig. 15. Here, the load value is optimal load. Fig. 15 shows that, as with a voltage source, the magnitude of the output power varies depending on the transmitter side circuit. It was found that high power was obtained on the transmitter side P, especially in P-N circuit. Here, using the approximation of equation (43) in Chapter 5 for the exact equation of the output power, it can be approximated as in Table 17. regardless of the transmission method. From the above, for both IPT and CPT, when a current source is connected, high power can be obtained by selecting P for the transmitter side circuit.

7.5 Summary of Transmission Characteristics The transmission characteristics of each circuit obtained from the above are summarized in Table 18 and 19. Here, Table 18. shows the table when the power supply is a voltage source and Table 19. shows the table when the power supply is a current source. The evaluation of the good points using ✓ marks shows that S-S in IPT is the best when the power supply is a voltage source and P-P in CPT is the best when the power supply is a current source.

Table 18. Summary of transmission characteristics. (voltage source)

Transmission Method	Circuit	Compensation Condition	CC/CV Characteristic	Optimal Load	Efficiency	Output Power	Number of ✓
IPT ✓long distance ✓low dielectric impact	N-N	Independent on k ✓	None	Middle	Middle	Low	1
	N-S	Independent on k ✓	None	Small	✓High	Middle	2
	N-P	Independent on k ✓	None	Large	✓High	Middle	2
	S-N	Independent on k ✓	✓CC	Middle	Middle	✓ Extra High	3
	P-N	Independent on k ✓	None	Middle	Middle	Low	1
	S-S	Independent on k ✓	✓CC	Small	✓High	✓High	✓4
	S-P	Depend on k	✓CV	Large	✓High	✓High	3
	P-S	Depend on k	✓CV	Small	✓High	Middle	2
	P-P	Depend on k	✓CC	Large	✓High	Middle	2
CPT ✓low cost ✓low metal impact ✓right weight	N-N	Independent on k ✓	None	Middle	Middle	Low	1
	N-S	Independent on k ✓	✓CC	Small	✓High	Middle	3
	N-P	Independent on k ✓	✓CC	Large	✓High	Middle	3
	S-N	Independent on k ✓	None	Middle	Middle	✓Extra High	2
	P-N	Independent on k ✓	None	Middle	Middle	Low	1
	S-S	Depend on k	✓CC	Small	✓High	✓High	3
	S-P	Depend on k	✓CV	Large	✓High	✓High	3
	P-S	Depend on k	✓CV	Small	✓High	Middle	2
	P-P	Independent on k ✓	✓CC	Large	✓High	Middle	3

Table 19. Summary of transmission characteristics. (current source)

Transmission Method	Circuit	Compensation Condition	CC/CV Characteristic	Optimal Load	Efficiency	Output Power	Number of ✓
IPT ✓long distance ✓low dielectric impact	N-N	Independent on k ✓	None	Middle	Middle	Low	1
	N-S	Independent on k ✓	✓CV	Small	✓High	Middle	3
	N-P	Independent on k ✓	✓CC	Large	✓High	Middle	3
	S-N	Independent on k ✓	None	Middle	Middle	Low	1
	P-N	Independent on k ✓	CC	Middle	Middle	✓Extra High	2
	S-S	Independent on k ✓	✓CV	Small	✓High	Middle	3
	S-P	Depend on k	✓CC	Large	✓High	Middle	2
	P-S	Depend on k	✓CC	Small	✓High	✓High	3
	P-P	Depend on k	✓CV	Large	✓High	✓High	3
CPT ✓low cost ✓low metal impact ✓right weight	N-N	Independent on k ✓	None	Middle	Middle	Low	1
	N-S	Independent on k ✓	None	Small	✓High	Middle	2
	N-P	Independent on k ✓	None	Large	✓High	Middle	2
	S-N	Independent on k ✓	✓CV	Middle	Middle	Low	2
	P-N	Independent on k ✓	✓CV	Middle	Middle	✓Extra High	3
	S-S	Depend on k	✓CV	Small	✓High	Middle	2
	S-P	Depend on k	✓CC	Large	✓High	Middle	2
	P-S	Depend on k	✓CC	Small	✓High	✓High	3
	P-P	Independent on k ✓	✓CV	Large	✓High	✓High	✓4

8. Comparison with Experiment

Experiments were carried out for measurements in a real environment. The parameters used are shown in Table 20 and 21. A vector network analyzer (VNA) was used for the measurements and the experimental environment is shown in Fig. 12. Here, in order to match k and Q in IPT and CPT, an external capacitor C_{1ex}, C_{2ex} are used in addition to the transmission capacitor in CPT.

The calculated and experimental results for efficiency and output power at different loads are shown in Fig. 16. S-S in IPT using a voltage source and P-P in CPT using a current source are shown here because of their excellent characteristics as shown in Chapter 7. For P-P in CPT, the output power connecting a current source was converted from the power supply current when a voltage source was connected.

Fig. 17 and 18 show the results: from Fig. 17, 18, it can be seen that the experimental and calculated results have a similar trend, so that the transmission characteristics presented in this paper are also the same in a real environment.

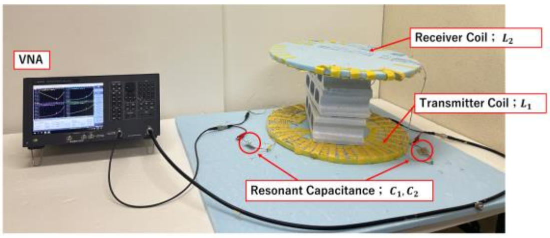

(h)IPT

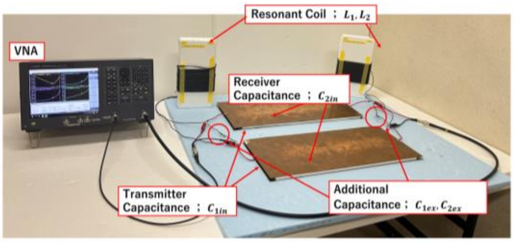

(h)CPT

Fig. 16 Experiment environment.

Table 20. Parameters of experiment in IPT

	Symbol	Value
Voltage Source	V_{in}	10 V
Coupling Coefficient	k	0.10
Resonant Frequency	f	85 kHz
Transmission Inductance	L_1, L_2	96.73 μH, 97.09μH
Internal Resistance	r_1, r_2	0.36 ohm, 0.46 ohm
Compensation Inductance	L_0, L_0'	98.76μH, 98.81μH
Internal Resistance	r_0, r_0'	0.38 ohm, 0.40 ohm
Resonant Capacitance	C_1, C_2	35.95 pF, 35.14 pF
Q value	Q_1, Q_2	142.39, 113.93

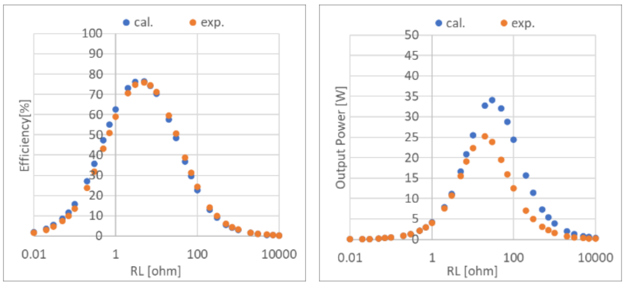

(a)Efficiency (h)Output Power

Fig. 17 Result of experiment in IPT.

Table 21. Parameters of experiment in CPT

	symbol	value
Current Source	I_{in}	1 A
Coupling Coefficient	k	0.08
Resonant Frequency	f	450 kHz
Transmission Capacitance	C_1, C_2	889.04 pF, 887.64 pF
Compensation Capacitance	C_0, C_0'	915.49 pF, 907.81 pF
Resonant Inductance	L_1, L_2	139.19 μH, 134.35 μH
Internal Resistance	r_1, r_2	2.44 ohm, 2.03 ohm
Q value	Q_1, Q_2	161.12, 186.85

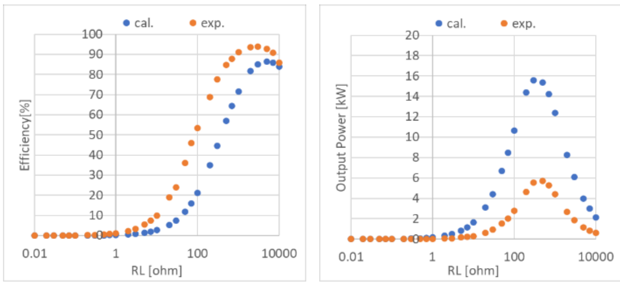

(a)Efficiency (h)Output Power

Fig. 18 Result of experiment in CPT.

9. Conclusion

In this paper, the transmission methods of the circuits consisting of non-resonant, series resonant and parallel resonant circuits of both IPT and CPT were compared in a systematic and fair. In terms of compensation condition and CC/CV characteristic, S-S in IPT and P-P in CPT are superior in that the compensation condition does not depend on the coupling coefficient and that they have gyrator characteristics, and a corresponding relationship can be found between them. In terms of optimal load and efficiency, IPT and CPT vary according to the circuit configuration on the receiver side, so for high efficiency transmission, it is suitable to use S or P for the receiver circuit. In terms of output power, which is also common to IPT and CPT, the magnitude of the output power varies depending on the transmitter side. Therefore, it is appropriate to select S for the transmitter side when using a voltage source, and P for the transmitter side when using a current source provides that high power. From the above it is concluded that S-S in IPT and P-P in CPT are superior.

References

(1) Y. H. Sohn, B. H. Choi, E. S. Lee, G. C. Lim, G. -H. Cho and C. T. Rim, "General Unified Analyses of Two-Capacitor Inductive Power Transfer Systems: Equivalence of Current-Source SS and SP Compensations," in IEEE Transactions on Power Electronics, vol. 30, no. 11, pp. 6030-6045, Nov. 2015

(2) H. Namiki, T. Imura and Y. Hori, "Magnetic Field Resonant Coupling in Wireless Power Transfer Comparison of Multiple Circuits Using LCL," 2022 IEEE 7th Southern Power Electronics Conference (SPEC), Nadi, Fiji, 2022, pp. 1-6

(3) A. Mahesh, B. Chokkalingam and L. Mihet-Popa, "Inductive Wireless Power Transfer Charging for Electric Vehicles–A Review," in IEEE Access, vol. 9, pp. 137667-137713, 2021

(4) Y. Li et al., "High Efficiency WPT System for Electric Vehicles with LCL-S and SS compensation," 2019 IEEE 4th International Future Energy Electronics Conference (IFEEC), Singapore, 2019, pp. 1-4

(5) S. Sasikumar and K. Deepa, "Comparative Study of LCL-S and LCC-S Topology of Wireless EV charging System," 2019 Innovations in Power and Advanced Computing Technologies (i-PACT), Vellore, India, 2019, pp. 1-6

(6) S. Cruciani, T. Campi, F. Maradei and M. Feliziani, "Simulation of Compensation Networks for a Transcutaneous WPT System to Achieve Compliance with ICNIRP Basic Restrictions," 2021 IEEE International Joint EMC/SI/PI and EMC Europe Symposium, Raleigh, NC, USA, 2021, pp. 381-385

(7) X. Dai, Y. Huang and Y. Li, "Topology comparison and selection of wireless power transfer system and parameter optimization for high voltage gain," 2017 IEEE PELS Workshop on Emerging Technologies: Wireless Power Transfer (WoW), Chongqing, China, 2017, pp. 1-5

(8) S. Luo, S. Li and H. Zhao, "Reactive power comparison of four-coil, LCC and CLC compensation network for wireless power transfer," 2017 IEEE PELS Workshop on Emerging Technologies: Wireless Power Transfer (WoW), Chongqing, China, 2017, pp. 268-271

(9) S. Kuroda and T. Imura, "Derivation and Comparison of Efficiency and Power in Non-resonant and Resonant Circuit of Capacitive Power Transfer," 2020 IEEE PELS Workshop on Emerging Technologies: Wireless Power Transfer (WoW), Seoul, Korea (South), 2020, pp. 152-157

(10) S. Kuroda and T. Imura, "Resonant circuit topology Comparison and CC / CV Characteristic Evaluation Considering the Difference in Power Supply in Capacitive Wireless Power Transfer circuits," IECON 2021 – 47th Annual Conference of the IEEE Industrial Electronics Society, Toronto, ON, Canada, 2021, pp. 1-5

(11) H. Namiki, T. Imura and Y. Hori, "Comparison of Multiple Circuits Including LCL in Inductive Power Transfer and Capacitive Power Transfer," IECON 2023- 49th Annual Conference of the IEEE Industrial Electronics Society, Singapore, Singapore, 2023, pp. 1-7

(12) L. Pamungkas, S. -H. Wu and H. -J. Chiu, "Equivalent Circuit Approach for Output Characteristic Design of Capacitive Power Transfer," in IEEE Transactions on Circuits and Systems II: Express Briefs, vol. 68, no. 7, pp. 2513-2517, July 2021

(13) Y. Wang, H. Zhang and F. Lu, "Review, Simulation, and Design of Four Basic CPT Topologies and the Application of High-Order Compensation Networks," in IEEE Transactions on Power Electronics, vol. 37, no. 5, pp. 6181-6193, May 2022

(14) B. Luo, L. Xu, T. Long, Y. Xu, R. Mai and Z. He, "An LC-CLC Compensated CPT System to Achieve the Maximum Power Transfer for High Power Applications," 2020 IEEE Applied Power Electronics Conference and Exposition (APEC), New Orleans, LA, USA, 2020, pp. 3186-3189

(15) S. Ning, J. Yang, Q. Zhu, M. Su, R. Tan and Y. Liu, "Comparative Simulation of LCL, LCLC, CLLC Compensation Networks for Capacitive Power Transfer," 2018 IEEE 4th Southern Power Electronics Conference (SPEC), Singapore, 2018, pp. 1-6

(16) C. Park, S. Lee, G. -H. Cho and C. T. Rim, "Innovative 5-m-Off-Distance Inductive Power Transfer Systems With Optimally Shaped Dipole Coils," in IEEE Transactions on Power Electronics, vol. 30, no. 2, pp. 817-827, Feb. 2015

(17) S. Y. Choi, J. Huh, W. Y. Lee and C. T. Rim, "Asymmetric Coil Sets for Wireless Stationary EV Chargers With Large Lateral Tolerance by Dominant Field Simulation," in IEEE Transactions on Power Electronics, vol. 29, no. 12, pp. 6406-6420, Dec. 2014

Hirono Namiki

(Non-Member) She entered the Department of Electrical Engineering, Faculty of Science and Technology, Tokyo University of Science in April 2018, graduated in March 2022, and entered the Department of Electrical Engineering, Graduate School of Science and Technology, Tokyo University of Science in April 2022. She is currently focusing on the unified theory of Inductive Power Transfer and Capacitive Power Transfer. She is a student member of the Institute of Electrical and Electronics Engineers (IEEE).

Takehiro Imura

(Member) Received the bachelor's degree in electrical and electronics engineering from Sophia University, Tokyo, Japan, in 2005, and the M.E. degree in electronic engineering and the D.Eng. degree in electrical engineering from The University of Tokyo, Tokyo, in 2007 and 2010, respectively. He joined the Department of Advanced Energy, Graduate School of Frontier Sciences, University of Tokyo, as a Research Associate, where since 2015, he has been a Project Lecturer. In 2019, he joined the Department of Electrical Engineering, Tokyo University of Science, as an Associate Professor. He is currently investigating wireless power transfer using magnetic resonant coupling and electric resonant coupling. His research interests include electric vehicle in-motion connected to renewable energy, sensors and cancer treatment. He is the winner of the IEEJ Industry Applications Society Distinguished Transaction Paper Award in 2015, of the IEEE Power Electronics Transactions First Prize Paper Award in 2017. He is a member of the Institute of Electrical and Electronics Engineers (IEEE), the Institute of Electronics, Information and Communication Engineers (IEICE), and the Society of Automotive Engineers of Japan (JSAE).

Yoichi Hori

(Fellow) Yoichi Hori received his B.S., M.S., and Ph.D. degrees in Electrical Engineering from the University of Tokyo, Tokyo, Japan, in 1978, 1980, and 1983, respectively. In 1983, he joined the Department of Electrical Engineering, The University of Tokyo, as a Research Associate. He later became an Assistant Professor, an Associate Professor, and, in 2000, a Professor at the same university. In 2002, he moved to the Institute of Industrial Science as a Professor in the Information and System Division, and in 2008, to the Department of Advanced Energy, Graduate School of Frontier Sciences, the University of Tokyo. He retired in March 2021, and has been in current position since April. Professor Emeritus of the University of Tokyo. From 1991-1992, he was a Visiting Researcher at the University of California at Berkeley. His research fields are control theory and its industrial applications to motion control, mechatronics, robotics, electric vehicles, etc. Recently, he has also been focusing on the research and promotion of wireless power transfer. He is a Life Fellow of IEEE (the Institute of Electrical and Electronics Engineers) and a past AdCom member of IES (Industrial Electronics Society). He has been the Treasurer of the IEEE Japan Council and Tokyo Section in a few years since 2001.